Stability analysis of high speed cutting in application to aluminum alloys

Analiza stabilności skrawania z dużą prędkością stopów aluminium

PAWEŁ BAŁON
EDWARD REJMAN
EVERT GEURTS
BARTŁOMIEJ KIEŁBASA
ROBERT SMUSZ
GRZEGORZ SZELIGA *

DOI: https://doi.org/10.17814/mechanik.2022.12.26

Progress in the production of cutting tools, CNC machine tools, and CAM software has contributed to improvement in subtractive machining processes, including milling, the so-called high speed cutting (HSC) and high performance cutting (HPC) machining. The cutting parameters that define the boundaries between the aforementioned technologies and conventional machining are not clearly defined. This is due to the close correlation between the process conditions and the types of processed material. High speed cutting and high performance cutting can be used for processing such as: machining of materials in the hardened state, machining without cutting fluid and with minimal lubrication, and thin-wall integral aerospace structures. The study examined complex analyses of HSC machining due to the process stability. The test results prove the dominant influence of cutting speed changes on a method's effectiveness for spindle speeds up to 80,000 rpm.
KEYWORDS: HSM, HSC, high speed milling, high speed cutting

Postęp w produkcji narzędzi skrawających, obrabiarek CNC oraz oprogramowania CAM przyczynił się do udoskonalenia procesów obróbki subtrakcyjnej, w tym frezowania, tzw. obróbki skrawaniem z dużą prędkością (HSC) oraz skrawania wysokowydajnego (HPC). Parametry skrawania, które wyznaczają granicę pomiędzy wymienionymi technologiami a obróbką konwencjonalną, nie są jednoznacznie określone. Wynika to ze ścisłej korelacji pomiędzy warunkami procesu a rodzajami obrabianego materiału. Skrawanie z dużą prędkością i wysokowydajne można stosować do: obróbki materiałów w stanie utwardzonym, obróbki na sucho i z minimalnym smarowaniem oraz do obróbki cienkościennych integralnych konstrukcji lotniczych. W pracy zbadano złożone analizy obróbki HSC pod względem stabilności procesu. Wyniki badań dowodzą dominującego wpływu zmian prędkości skrawania na skuteczność metody dla prędkości obrotowych wrzeciona do 80000 obr/min.
SŁOWA KLUCZOWE: HSM, HSC, frezowanie z dużą prędkością, skrawanie z dużą prędkością

Nomenclature

f_z – feed per tooth [mm/obr]
f_o – natural frequency of the system [s^{-1}]
a_p – cutting depth [mm]
n – spindle rotational speed [obr/min]
f_{ds} – frequency of self-excited vibrations [Hz]
N_z – number of cutter teeth
R_a – surface roughness parameters, arithmetic means deviation from the mean line [μm]
S_a – surface roughness parameters, arithmetic surface deviation from reference surface [μm]
f_m – minute feed [mm/obr]
$F_x x(t)$ – forced vibrations
t – time [s]
m – mass [kg]
c, k – variables

Greek symbols

x – amplitude
n_s – frequency of self-excited vibrations [s^{-1}]
v_c – cutting speed [m/min], [m/s]

Subscripts

HSC – high speed cutting
HPC – high performance cutting
MHWT – machine tool–holder–workpiece–tool
MDS – mass-dissipation-elastic system
DLC – diamond-like carbon
VHM – vollhartmetal

Introduction

High speed cutting (HSC) and high performance cutting (HPC) allow you to shorten machining time by more than 30%, increase machining efficiency, reduce the cutting force, and obtain a better quality of the

* Dr inż. Paweł Bałon – balonpawel@gmail.com, https://orcid.org/0000-0003-3136-7908 – Akademia Górniczo-Hutnicza im. Stanisława Staszica w Krakowie, WIMiR, Kraków, Poland; SZEL-TECH, Mielec, Poland
Dr inż. Edward Rejman – erejman@prz.edu.pl, https://orcid.org/0000-0003-4716-7613 – Politechnika Rzeszowska im. Ignacego Łukasiewicza, Rzeszów, Poland; SZEL-TECH, Mielec, Poland
Ir. E.G.M. Evert Geurts – evert.geurts@nlr.nl, 0000-0001-8345-1429 – Royal NLR, Marknesse, The Netherlands
Mgr inż. Bartłomiej Kiełbasa – bartek.kielbasa@gmail.com, https://orcid.org/0000-0002-3116-2251– SZEL-TECH, Mielec, Poland
Dr hab. inż. Robert Smusz – robsmusz@gmail.com, https://orcid.org/0000-0001-7369-1162 – Politechnika Rzeszowska im. Ignacego Łukasiewicza, Rzeszów, Poland; SZEL-TECH, Mielec, Poland
Grzegorz Szeliga – g.szeliga@szel-tech.com – SZEL-TECH, Mielec, Poland

machined surface. The advantages of high speed machining also include: reduced burr formation, improved chip evacuation, and increased process stability. Comparing both technologies, it can be concluded that when cutting high performance (HPC) higher values of cutting depth a_p, milling width a_e and feed per tooth f_z are both used at a lower cutting speed v_c. On the other hand, HSC machining is characterized by a higher cutting speed v_c and smaller sections of the cutting layer. For HSC and HPC, there are also different conditions of contact between the cutting edges of the tools and the workpiece. With HPC, the mentioned contact angle of up to 180° causes the blades to heat up to an extreme degree and therefore it is justified to use a lower cutting speed v_c compared to HSC machining, for which the contact angle is much smaller and amounts to approx. 30°. In addition, a significantly worse surface quality is obtained after cutting with high-performance HPC. The occurrence of self-excited vibrations, as a rule, makes machining practically impossible because it causes significant surface roughness, severe wear of the blade and machine tool elements, and often unbearable noise, as well. Hence, avoiding such vibrations is essential. This can be achieved by:

- selection of stable machining conditions,
- adjusting for areas of stable work between bag curves,
- significant reduction of the cutting speed,
- configuration of the stiffness of the MHWT system,
- use of passive or active vibration dampers,
- reducing the number of teeth in cutters.

Another very important factor in limiting self-excited vibrations is the adjusting for stable rotational speeds of the machining tool, which is important when using HSM machining. After some simplification, this frequency of vibrations can be determined from the formula (1) [8–10, 14]:

$$n_s = \frac{60\, f_{ds}}{N_z} \tag{1}$$

where: f_{ds} – frequency of self-excited vibrations, N_z – number of cutter teeth.

Assuming the rotational speed determined from formula (1) allows you to search for stable rotational speeds of the tool. The self-excited vibration frequency f_{ds} necessary to use the presented method can be determined from any available signal collected during the test, for example, cutting force measurement. The application of formula (1) is possible, assuming that the natural frequency of the system f_o is approximately equal to the frequency of forced vibrations.

The dynamics of the machining process

Modern metalworking machine tools are relatively stiff. Due to the design and overall dimensions resulting from the size of the workpieces, this stiffness is limited. Hence, during the machining process, vibrations may appear, and the extent to which they occur largely depends on the combined stiffness of the MHWT systems (machine tool – holder – workpiece – tool). Self-excited vibrations are particularly disadvantageous. They cause characteristic machining traces on the machined surface (fig. 1), accelerated wear of the machine tool and the tool blade, and even their eventual breakage and consequent destruction.

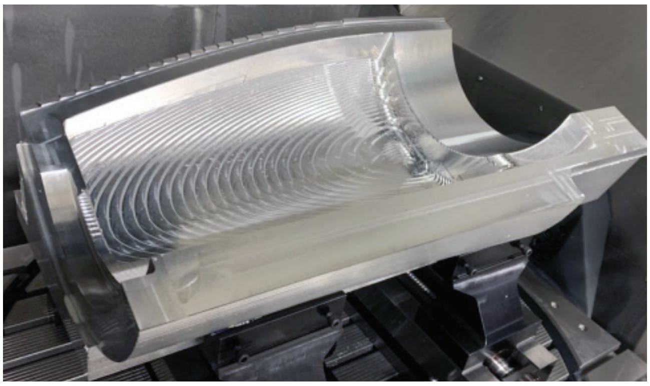

Fig. 1. Surface machined by milling with self-excited vibrations

Due to self-excited vibrations, high-performance machining and high-speed machining are limited. Self-excited vibrations occur when there is no influence on the exciting force system. Their characteristic feature is that the variable force supplying energy to the vibrating system is caused by the vibrations themselves. According to the terminology used in the dynamics of machine tools, the dynamic MHWT system consists of: mass-dissipation-elastic system (MDS) and work processes. Hence, for example, the equation of motion of the MDS system with one degree of freedom, in which self-excited vibrations occur takes the form:

$$m\ddot{x}(t) + c\dot{x}(t) + kx(t) = F_x[x(t)] \tag{2}$$

Should the vibrations stop for any reason, the supporting force will also disappear. In order for self-excited vibrations to arise, there must be a mechanism causing a feedback between the vibrations of the MDS system and the force acting on the system. The frequency of self-excited vibrations is similar to the natural frequency of the MDS system. The amplitude of these vibrations in a linear system (equation 2) grows to infinity. In practice, an increase in amplitude always leads to an overflow of the linearity range of the system and, for example, the elasticity and damping coefficients increase along with an increase of the deflection from the equilibrium state. This causes the amplitude of self-excited vibrations to be established. A system in which self-excited vibrations occur is considered unstable: the stability of the system is called its resistance to the formation of self-excited vibrations within it. Basic vibration characteristics are shown in fig. 2.

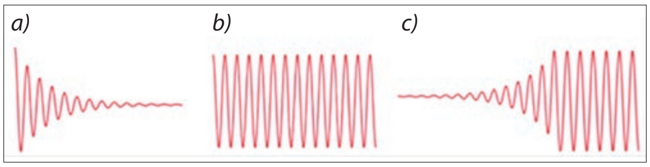

Fig. 2. Basic characteristics and waveforms of vibrations: *a)* free, *b)* forced, and *c)* self-excited [16]

Milling process stability studies

Our own tests conducted under laboratory and production conditions confirmed the potential for instability in the milling process, manifested by the occurrence of vibrations, especially of machining tools, and deterioration of the machined surface's quality, requiring additional finishing. It was especially visible when processing shaped surfaces with large curvature gradients. In connection with the above, our own research was carried out. The tests were carried out on the stand shown in fig. 3. The subjects of the tests were samples made of materials in the 70XX aluminum alloys group, which have good strength properties and are widely used in the aviation industry. Two grades of alloys were selected, namely alloys 7050 and 7075. These alloys, apart from their high strength properties, are conducive to machining and allow for the use of high cutting parameters [4, 11].

Particular attention was paid to the selection of tools. A VHM MTC DLC end mill tool with diameters of ⌀8 mm and ⌀16 mm was used. The tools had the latest generation DLC-sp2 coating. The milling cutter had eccentric grinding and polished chip flutes in order to ensure good removal of chips generated during machining. When machining aluminum alloys, especially the turning and drilling processes a long ribbon chip is produced. For both tools, the tests were carried out for different toolholder lengths: 70 and 160 mm.

Due to the fact that the tool shift in the direction of the *Y* axis (standard axis designation) of the tested machine was obtained by moving the headstock, the tests were carried out in two ways, i.e. both for its minimum and maximum stroke. The tests were carried out for two milling widths a_e equal to the 0.75 milling cutter diameter. The test stand is shown in fig. 3. Examples of test results illustrating the stability of the milling process are shown in figs 4 and 5.

The conducted tests allowed for the determination of the so-called bag curves for the machine tool used, tools used, and the size of their overhang. These curves show the relationship between the depth of cut a_p and the rotational speed of the milling cutter n. Based on the graphs obtained, the areas of permissible work can be estimated dynamically. Above the curve,

Fig. 3. Stand for testing the stability of the milling process: tools with a vibration sensor mounted on the machine tool

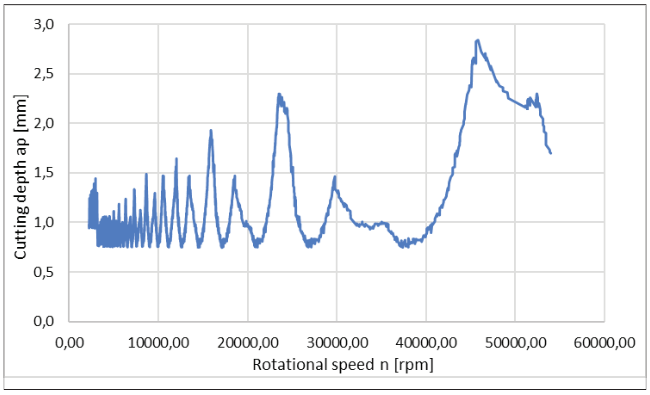

Fig. 4. Milling stability chart: material aluminum alloy 7050, milling cutter ⌀8 mm, milling width $a_e = 3$ mm, feed per tooth $f_z = 0.07$ mm, and minimum headstock stroke

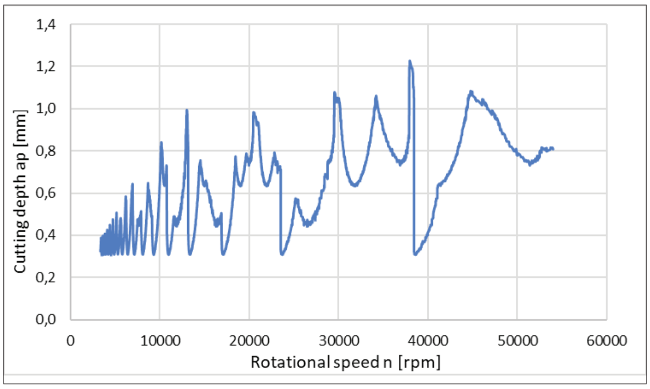

Fig. 5. Milling stability diagram: material aluminum alloy 7050, milling cutter ⌀8 mm, milling width $a_e = 4$ mm, feed per tooth $f_z = 0.07$ mm, and maximum headstock stroke

we are dealing with an unstable work area, where self-excited vibrations occur, which cause the tool or the workpiece to vibrate when the tool starts to feed. The stable system is free from vibrations depending on the combination of the spindle speed n, depth of cut a_p, width of the cutting layer a_e. Such an analysis is possible for each selected combination of tools, their diameter, method of clamping and cutting parameters. Increasing the depth of cut and the amount of tool stroke significantly narrows the areas of stable work and requires detailed research to ensure stable machining areas. The area of stable work expands as the rotational speed of the tool is increased, which is particularly advantageous when using HSM machining.

As described by the formula (1), the determination of the spindle rotational speed n_s requires knowledge of the self-excited vibration frequency f_{ds} of the MHWT system. This frequency [16], with some simplification, can be determined on the basis of any available bound signal with the machining process on the machine tool, for example cutting force, vibration, or sound intensity.

However, it should be remembered that during milling, these signals are largely influenced by vibrations caused by the impact of the blades. Therefore, the frequencies of forced vibrations should be identified on the basis of the rotational speed of the spindle and the number of teeth of the tool, and then negligible factors should be omitted. For our research, a portable device of the Microlog CMVA 60 type was used (fig. 6).

Fig. 6. Test apparatus, type Microlog CMVA 60 for measuring spindle vibrations during machining with rotational speeds of $n = 20{,}000 \div 80{,}000$ rpm

Thanks to having a number of functions, it allowed us to not simply collect vibration data; it also includes an intelligent system that allows detection, analysis of frequencies, and editing of files downloaded from the machine.

The dynamic tests of the cutting process were carried out for spindle rotational speeds $n = 40{,}000$; 60,000; and 80,000 rpm. The tests were carried out both in free running (without loading the spindle with cutting forces) and under load. The machining was performed with a minute feed $f_m = 100$ mm/min and cutting depths a_p equal to 0.05; 0.10; and 0.15 mm. The radial runout of the unloaded tool was 0.02 mm. The results of the tests carried out are shown in the stability diagrams. The obtained test results made it possible to indicate safe (stable) areas of spindle operation with selected machining parameters, especially the dominant vibration frequencies and the corresponding vibration amplitude velocity. These parameters should be particularly preferred during finishing. The exemplary results of the conducted tests are shown in fig. 7.

The obtained test results allowed us to indicate safe areas of the spindle operation with selected machining parameters, especially the dominant vibration frequencies and the corresponding amplitude velocities. These parameters should be especially preferable during machining. The highest spindle vibration amplitude velocities occurred at the spindle rotational speed of $n = 40{,}000$ rpm. The increase in the spindle speed resulted in a decrease in the amplitude speed. The increase in the spindle load (greater cutting depth a_p) resulted in an increase in the amplitude of the vibration frequency. When conducting dynamic tests, the quality of the samples processed with the face of the cutter was also assessed during the processing of flat surfaces. The performed treatment allowed us to obtain surface roughness determined by the Ra parameter, from $R_a = 0.078$ µm for the cutting speed $v_c = 1507$ m/min to $R_a = 0.14$ µm for $v_c = 753.6$ m/min. In the case of processing flat surfaces with the side surface of the cutter, the surface roughness is greater. For the treatment of such surfaces with a cutting speed of $v_c = 1507$ m/min, a roughness of $R_a = 0.22$ µm was obtained.

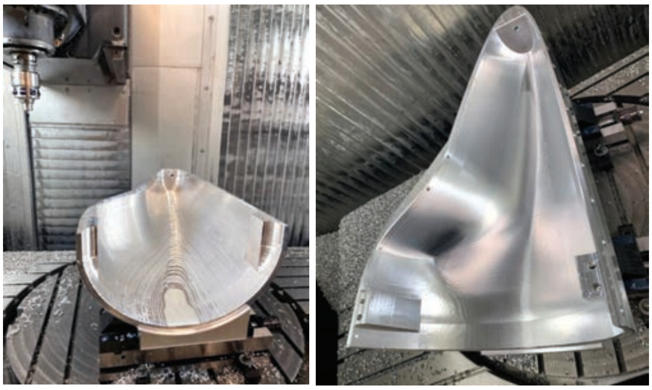

Fig. 7. Stability of the milling process during HSC machining of an aircraft structure element

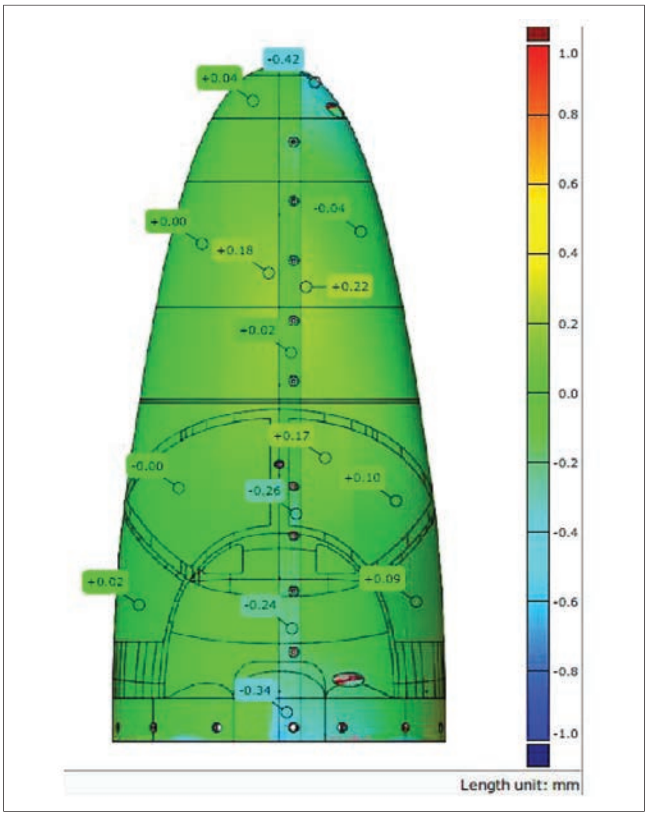

Fig. 8. Map of deviations of the dimensions of the machined surface in relation to the theoretical 3D model consisting of two symmetrical halves

For the practical application of the research, the elements used in the project (No. 821038, H2020-CS2-CFP07-2017-02) were processed, the structural elements used in the construction of the aircraft engine housing model were intended for aerodynamic tests made of AW aluminum alloy 6082 (PA4), as shown in fig. 7. The machining was carried out in two main operations: shaping machining and finishing machining. The completed casing was subjected to dimensional verification using a 3D scanner and obtaining a map of deviations from the theoretical model (fig. 8). The obtained dimensions allowed us to conclude that the manufactured model is within the assumed tolerances of ±0.3 mm. The performed finishing allowed for attainment of surface roughness at the S_a level, equal to 0.32 µm (S_a – arithmetic mean of the surface deviation from the mean reference surface).

Conclusions

The conducted research allowed us to confirm the assumptions that it is possible to shape complex aircraft structures using the HSM milling method and obtain satisfactory results, both in terms of the roughness of the machined surface as well as its linear dimensions. In the treatment of test specimens, it is possible to obtain a cutting speed of v_c = 1500 m/min, and in the treatment of real structures v_c = 800 m/min, which is associated with the possibility of damaging the tool and destroying the expensive blank. The obtained surface roughness corresponds to the roughness obtained during grinding. HSM technology allows one to dispense with grinding. The obtained research results in the field of cutting process dynamics allow one to determinate the dangerous work areas of the machine tool spindle and to adjust them in such a way as to avoid self-excited vibrations and deteriorate the quality of the machined surface.

In the conducted tests, the highest vibration amplitude velocities, and thus also the occurrence of resonance, occurred at the spindle speed of n = 40,000 rpm, the cutting depth a_p = 0.15 mm and the minute feed f_m = 100 mm/min. The increase in the spindle rotational speed n caused a decrease in the speed of the spindle vibration amplitude. The increase in the spindle load (cutting force) increased the speed of the cutting tool's vibration amplitude.

Acknowledgements

This research was conducted within the project "High Speed Civil Tilt Rotor Wind Tunnel Project (HIGHTRIP)". Grant agreement no.: 821038, H2020-CS2-CFP07-2017-02, co-financed by Horizon 2020 Clean Sky 2. Partners: Stichting Natonaal Lucht – en Ruimtevaartlaboratorium (NLR), Łukasiewicz Reseach Network – Institute of Aviation (ILOT), Szel-Tech Szeliga Grzegorz, P.W. „Metrol" Dariusz Dąbkowski, Leonardo S.p.a.

REFERENCES

[1] Shamsuddin K.A., Ab-Kadir A.R., Osman M.H. "A Comparison of Milling Cutting Path Strategies for Thin Walled Aluminium Alloys Fabrication". *The International Journal Of Engineering And Science* (IJES). 2, 3 (2013): 01–08.

[2] Awan W.S., Mabrouki T. "Numerical and experimental investigations of post-machining distortions in thin machined structures considering material-induced residual stress". *Journal of the Brazilian Society of Mechanical Sciences and Engineering*. 39 (2017): 509–521, https://doi.org/10.1007/s40430-015-0386-5.

[3] Seguy S., Campa F.J., Lopez de Lacalle L.N., Arnaud L., Dessein G., Aramendi G. "Toolpath dependent stability lobes for the milling of thin-walled parts". *International Journal of Machining and Machinability of Materials*. 4, 3–4 (2008): 261–274, https://doi.org/10.1504/IJMMM.2008.023720.

[4] Bałon P., Rejman E., Smusz R., Kiełbasa B. „Obróbka z wysokimi prędkościami skrawania cienkościennych konstrukcji lotniczych". *Mechanik*. 8–9 (2017): 726–729, https://doi.org/10.17814/mechanik.2017.8-9.105.

[5] Adamski W. „Wybrane kierunki zwiększania wydajności procesów skrawania". *Mechanik*. 5–6 (2009): 540–546.

[6] Kuczmaszewski J., Łogin W., Pieśko P., Zagórski I. "State of Residual Stresses after the Process of Milling Selected Aluminium Alloys". *Advances in Science and Technology. Research Journal*. 12, 1 (2018): 63–73, https://doi.org/10.12913/22998624/81768.

[7] Tang Z.T., Liu Z.Q., Pan Y.Z., Wan Y., Ai X. "The influence of tool flank wear on residual stresses induced by milling aluminum alloy". *Journal of Materials Processing Technology*. 209, 9 (2009): 4502–4508, https://doi.org/10.1016/j.jmatprotec.2008.10.034.

[8] Adamski W. „Analiza przyczyn zmiany kształtu części lotniczych podczas obróbki skrawaniem na maszynach CNC i skuteczne przeciwdziałanie tym zjawiskom". *Mechanik*. 1 (2012).

[9] Zębala W. „Minimalizacja błędów obróbki przedmiotów cienkościennych". *Inżynieria Maszyn*. 15, 3 (2010): 45–54, bwmeta1.element.baztech-article-LOD9-0021-0028.

[10] Jemielniak K. „*Obróbka skrawaniem podstawy, dynamika, diagnostyka*". Warszawa: Oficyna Wydawnicza Politechniki Warszawskiej (2018).

[11] Bałon P., Rejman E., Kiełbasa B., Smusz R. "Using HSM technology in machining of thin-walled aircraft structures". *Acta Mechanica et Automatica*. 16, 1 (2022): 27–33, https://doi.org/10.2478/ama-2022-0004.

[12] Bałon P., Rejman E., Kiełbasa B., Smusz R., Światoniowski A., Szostak J., Kowalski Ł., Cieślik J. "*The application of thin-walled integral constructions in aviation as exemplified by the SAT-AM project*". MATEC, 2019.

[13] Wade A. "Cut the chatter". *Cutting Tool Engineering* (2015), https://www.ctemag.com/news/articles/cut-chatter, (access: 1st October 2022).

[14] Morita H., Yamashita T. "Tracing and visualizing variation of chatter for in-process identification of preferred spindle speeds". *Procedia CIRP*. 4 (2012): 11–16, https://doi.org/10.1016/j.procir.2012.10.003.

[15] Cichosz P., Kuzinovski M. „*Ekonomiczne aspekty doboru narzędzi skrawających do zadania produkcyjnego. Obróbka skrawaniem: wysoka produktywność*". Wrocław: Oficyna Wydawnicza Politechniki Wrocławskiej (2007).

[16] Cichosz P., Kuzinovski M. „*Sterowane i mechatroniczne narzędzia skrawające*". Warszawa: PWN, 2016.

[17] Bałon P., Rejman E., Kiełbasa B., Smusz R., Światoniowski A., Szostak J., Kowalski Ł., Cieślik J. "Thin-walled integral constructions in aircraft industry". *Procedia Manufacturing*. 47 (2020): 498–504, https://doi.org/10.1016/j.promfg.2020.04.15